J. Fluid Mech. (2012), *vol.* 708, *pp.* 596–606. © Cambridge University Press 2012
doi:10.1017/jfm.2012.349

The efficiency of an array of tidal turbines partially blocking a wide channel

Takafumi Nishino† and Richard H. J. Willden

Department of Engineering Science, University of Oxford, Parks Road, Oxford OX1 3PJ, UK

(Received 28 March 2012; revised 21 May 2012; accepted 3 July 2012; first published online 20 August 2012)

A new theoretical model is proposed to explore the efficiency of a long array of tidal turbines partially blocking a wide channel cross-section. An idea of scale separation is introduced between the flow around each device (or turbine) and that around the entire array to assume that all device-scale flow events, including 'far-wake' mixing behind each device, take place much faster than the horizontal expansion of the flow around the entire array. This assumption makes it possible to model the flow as a combination of two quasi-inviscid problems of different scales, in both of which the conservation of mass, momentum and energy is considered. The new model suggests the following: when turbines block only a small portion of the span of a shallow channel cross-section, there is an optimal intra-turbine spacing to maximize the efficiency (limit of power extraction) for a given channel height and width. The efficiency increases as the spacing is reduced to the optimal value due to the effect of local blockage, but then decreases as the spacing is further reduced due to the effect of array-scale choking, i.e. reduced flow through the entire array. Also, when the channel is infinitely wide, the efficiency depends solely on the local area blockage rather than on the combination of the intra-turbine spacing and the channel height. As the local blockage is increased, the efficiency increases from the Lanchester–Betz limit of 0.593 to another limiting value of 0.798, but then decreases as the local blockage is further increased.

Key words: channel flow, coastal engineering, shallow water flows

1. Introduction

The limit of power extraction by a turbine in a tidal channel is significantly affected by its channel blockage ratio, i.e. the ratio of the frontal projected area of the turbine to the channel cross-sectional area (Garrett & Cummins 2007; Houlsby *et al.* 2008; Whelan, Graham & Peiró 2009). Garrett & Cummins (2007) used a one-dimensional quasi-inviscid model to show that the limit of power extraction by a single turbine in a channel of uniform cross-sectional area is proportional to $(1-B)^{-2}$, where B is the blockage ratio. Their model assumed that viscous (or turbulent) mixing behind the turbine takes place only downstream of the location where the pressure equilibrates across the channel cross-section. The actual limit can be even higher due to turbulent mixing just downstream of the turbine (i.e. upstream of the pressure equilibrium location) as the turbulent shear stress acts in such a way as to accelerate the turbine wake and decelerate the flow surrounding the wake (Nishino & Willden 2012). Nevertheless, the one-dimensional quasi-inviscid model agrees fairly well with

† Email address for correspondence: takafumi.nishino@eng.ox.ac.uk

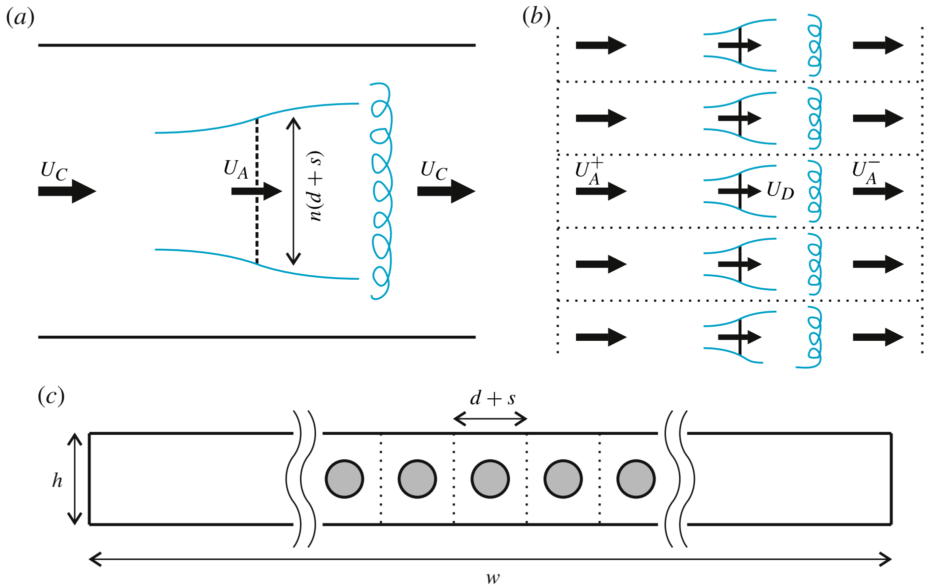

FIGURE 1. (Colour online) Schematic of the turbine array model: (*a*) array-scale flow expansion and mixing; (*b*) device-scale flow expansion and mixing; and (*c*) cross-sectional view of the channel.

three-dimensional actuator disk computations, provided that the mixing just downstream of the turbine is not significant.

For the development of practical tidal power generation systems making a meaningful contribution to the future energy supply, it is necessary to consider the efficiency of a number of turbines installed in a large tidal channel. The quasi-inviscid model of Garrett & Cummins (2007) suggests that the efficiency (limit of power extraction) increases as the channel blockage is increased by installing more and more turbines across the channel cross-section. In reality, however, the efficiency is expected to decrease if too many turbines are installed as their hydrodynamic drag becomes significant compared to the drag along the (undisturbed) channel itself and hence the energy flux through the channel is reduced (Garrett & Cummins 2005). Recently, Vennell (2010) combined these two effects (namely the cross-sectional blockage effect and the channel choking effect) in his tidal farm model, which explored the efficiency of a number of turbines homogeneously arrayed across the channel cross-section and at several streamwise locations of the channel. Vennell (2011) further extended his tidal farm model to account for the effect of non-uniformity of the channel cross-section.

In this study we extend the model of Garrett & Cummins (2007) in a different direction from the tidal farm model of Vennell (2010, 2011). Specifically, we consider the efficiency of a partial tidal fence, i.e. a row of a number of turbines arrayed only across a part of a wide channel cross-section rather than the entire cross-section (figure 1). This flow configuration is closely related to a practical situation where a considerable portion of a tidal channel cross-section needs to be unblocked to allow for navigation of vessels and so forth. We first consider the separation of the scales of flow around each turbine and that around a large array, followed by the introduction of three different channel blockage definitions (namely the local, array and global blockages). These concepts result in a new tidal turbine array model, which theoretically explores the effects of channel height, width and intra-turbine spacing on the efficiency of a partial tidal fence.

In the present study, we assume that the mass flux through the channel is constant in order to simplify the problem and thus focus on the combined effects of local and global blockages in an ideal tidal channel situation. These combined effects are of fundamental importance for understanding the efficiency of a partial tidal fence and are theoretically explored for the first time in this paper. It should be borne in mind that, in a practical tidal channel situation, the above assumption may not fully hold as the hydrodynamic drag induced by the installation of the turbine array may become significant compared to the drag along the entire channel. For such a case, a further extension of the model would be required to take account of the channel choking effect, perhaps in a similar way to the model of Vennell (2010) for homogeneously distributed turbines. It should also be noted that the present model does not account for the effect of changes in water depth, which has been previously discussed, e.g. by Houlsby *et al.* (2008), Whelan *et al.* (2009) and Draper *et al.* (2010).

2. Model

Consider a large number (n) of turbine rotors of diameter d arrayed in a rectangular channel of uniform height h and width w (figure 1). The intra-turbine spacing, s, is constant along the array; hence the spanwise length or width of the array is $n(d+s)$. As with the model of Garrett & Cummins (2007), the flow through the channel is assumed to be incompressible and inviscid except for the far-wake region where mixing is allowed (discussed later). The flow speed far upstream of the array is uniform and identical to the channel cross-sectional average of the streamwise velocity, U_C, which is fixed in the present model.

To theoretically explore the efficiency of this partial tidal fence, we first consider the separation of the scales of flow around each device (or turbine) and that around the entire array (or fence). Since the scale of (three-dimensional) flow around each turbine is related to the rotor diameter d whereas the scale of (quasi-two-dimensional) flow around the entire array is related to the array width $n(d+s)$, all device-scale flow events around each device (including 'far-wake' mixing behind each device) take place much faster than the horizontal expansion of the flow around the entire array when the number of turbines (n) is sufficiently large. This scale separation makes it possible to model this flow system as a combination of two quasi-inviscid problems of different scales; namely the array-scale (figure 1*a*) and device-scale (figure 1*b*) problems, to both of which the model of Garrett & Cummins (2007) is applicable.

For the array-scale problem, the flow through the channel is assumed to be two-dimensional (as the channel height h is significantly smaller than its width w) and the array is considered as a single power-extracting fence of height h and width $n(d+s)$, blocking the channel cross-section entirely in the vertical direction but only partially in the spanwise direction. Here we define the array blockage, B_A, as

$$B_A = \frac{\text{(representative) array area}}{\text{channel cross-sectional area}} = \frac{hn(d+s)}{hw} = \frac{1+\dfrac{s}{d}}{\dfrac{w}{nd}}, \tag{2.1}$$

where s/d and w/nd are non-dimensionalized intra-turbine spacing and channel width, respectively. Following the model concept of Garrett & Cummins (2007), the streamwise velocity at the fence, U_A, is assumed to be uniform across the fence, i.e.

we assume that the array end effects are negligible. (From a practical point of view, a key question here is how large the number of turbines, n, needs to be to satisfy this assumption; this is an open question and is the subject of ongoing investigation.) The array-scale mixing is assumed to take place only downstream of the location where the pressure equilibrates across the entire channel cross-section. Following the array-scale mixing, the flow speed returns to U_C far downstream of the array. It should be noted that here we implicitly assume that the channel is long enough to accommodate the array-scale mixing; hence the channel length is long compared to the array wake length, which itself is long compared to the array width.

Meanwhile, for the device-scale problem, we consider n identical rectangular flow passages of height h and width $d+s$ arrayed in parallel across the entire array span. The streamwise length of each passage is long enough to contain all device-scale flow events but still negligibly short compared to the scale of horizontal flow expansion around the entire array. Hence the flow speed at the inlet of each local flow passage, U_A^+, is assumed to be identical to U_A used in the array-scale problem. Each device blocks a part of the cross-section of local flow passage; the local blockage, B_L, is therefore defined as

$$B_L = \frac{\text{single device area}}{\text{local passage cross-sectional area}} = \frac{\dfrac{\pi d^2}{4}}{h(d+s)} = \frac{\pi}{4\dfrac{h}{d}\left(1+\dfrac{s}{d}\right)}, \tag{2.2}$$

where h/d is a non-dimensionalized channel height. Here the global blockage, B_G, may also be defined as

$$B_G = \frac{\text{total device area}}{\text{channel cross-sectional area}} = \frac{n\dfrac{\pi d^2}{4}}{hw} = \frac{\pi}{4\dfrac{h}{d}\dfrac{w}{nd}}. \tag{2.3}$$

Note that $B_G = B_L B_A$. Again following the concept of Garrett & Cummins (2007), it is assumed that the streamwise velocity at the device, U_D, is uniform across the device area, and the (device-scale) mixing takes place only downstream of the location where the pressure equilibrates across the cross-section of each local flow passage. The flow speed at the outlet of the local flow passage, U_A^-, is uniform and identical to U_A used in the array-scale problem, provided that the number of turbines (n) is sufficiently large.

Similarly to the three different blockages defined above, three different axial induction factors are also defined as follows:

$$a_L = 1 - \frac{U_D}{U_A}, \quad a_A = 1 - \frac{U_A}{U_C}, \quad a_G = 1 - \frac{U_D}{U_C}. \tag{2.4}$$

Note that $(1-a_G) = (1-a_L)(1-a_A)$.

The array-scale and device-scale problems described above are solved simultaneously by considering that the thrust force on the entire array (obtained from the array-scale problem) is n-times larger than that on each device, T_D (obtained from the device-scale problem). Using q and ρ to denote dynamic pressure and fluid density, respectively, we define three different thrust coefficients, namely the local (C_{TL}), array

(C_{TA}) and global (C_{TG}) thrust coefficients:

$$C_{TL} = \frac{\text{thrust on single device}}{\text{local inlet } q \times \text{single device area}} = \frac{T_D}{\dfrac{1}{2}\rho U_A^2 \dfrac{\pi d^2}{4}}, \tag{2.5}$$

$$C_{TA} = \frac{\text{thrust on array}}{\text{channel inlet } q \times \text{array area}} = \frac{nT_D}{\dfrac{1}{2}\rho U_C^2 hn(d+s)} = (1-a_A)^2 B_L C_{TL}, \tag{2.6}$$

$$C_{TG} = \frac{\text{total thrust on } n \text{ devices}}{\text{channel inlet } q \times \text{total device area}} = \frac{nT_D}{\dfrac{1}{2}\rho U_C^2 n \dfrac{\pi d^2}{4}} = (1-a_A)^2 C_{TL}. \tag{2.7}$$

Also, three different power coefficients, namely the local (C_{PL}), array (C_{PA}) and global (C_{PG}) power coefficients, are defined as

$$C_{PL} = \frac{P_D}{\dfrac{1}{2}\rho U_A^3 \dfrac{\pi d^2}{4}}, \quad C_{PA} = (1-a_A)^3 B_L C_{PL}, \quad C_{PG} = (1-a_A)^3 C_{PL}, \tag{2.8}$$

where $P_D = T_D U_D$ is the power extracted by each device.

Following Garrett & Cummins (2007), we first consider the conservation of mass, momentum and energy in each local flow passage to obtain C_{TL} as a function of the local induction factor, a_L, and blockage, B_L (see also Houlsby *et al.* 2008):

$$C_{TL} = (1-\gamma_L)\left[\frac{(1+\gamma_L) - 2B_L(1-a_L)}{(1-B_L(1-a_L)/\gamma_L)^2}\right], \tag{2.9}$$

where γ_L, which is the ratio of the device wake velocity (at the device-scale pressure equilibrium location) to U_A, is also related to a_L and B_L as

$$(1-a_L) = \frac{1+\gamma_L}{(1+B_L) + \sqrt{(1-B_L)^2 + B_L(1-1/\gamma_L)^2}}. \tag{2.10}$$

Note that C_{PL} is also obtained by $C_{PL} = (1-a_L)C_{TL}$ at this stage; however, C_{TA}, C_{TG}, C_{PA} and C_{PG} are still unknown as they depend on the array induction factor a_A.

Next, we consider the conservation of mass, momentum and energy in the array-scale problem. In analogy with the derivation of C_{TL} (2.9), C_{TA} is obtained as a function of the array induction factor, a_A, and blockage, B_A:

$$C_{TA} = (1-\gamma_A)\left[\frac{(1+\gamma_A) - 2B_A(1-a_A)}{(1-B_A(1-a_A)/\gamma_A)^2}\right], \tag{2.11}$$

where γ_A, which is the ratio of the array wake velocity (at the array-scale pressure equilibrium location) to U_C, is also related to a_A and B_A as

$$(1-a_A) = \frac{1+\gamma_A}{(1+B_A) + \sqrt{(1-B_A)^2 + B_A(1-1/\gamma_A)^2}}. \tag{2.12}$$

Equations (2.9) and (2.11) present thrust coefficients for the local- and array-scale problems as a function of induction factor and blockage for each problem. Equation (2.6) provides the coupling between the two problems, i.e. C_{TA} obtained from the array-scale problem (2.11) needs to agree with C_{TA} from (2.6), where C_{TL} is obtained from the device-scale problem (2.9). Since the former (array-derived) C_{TA}

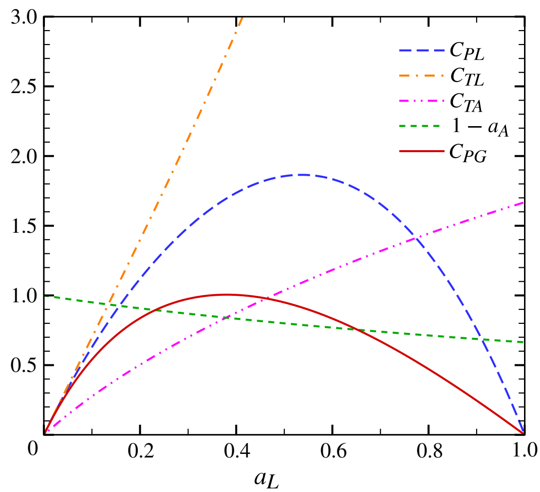

FIGURE 2. (Colour online) Influence of the local axial induction factor a_L for a high local blockage case ($w/nd = 5$, $h/d = 1.2$, $s/d = 0.5$, $B_L = 0.436$, $B_A = 0.3$, $B_G = 0.131$).

increases whilst the latter (device-derived) C_{TA} decreases as a_A increases, the value of a_A that yields the same C_{TA} for the local- and array-scale problems is uniquely determined for a given a_L. Eventually, all thrust and power coefficients defined above are uniquely determined (numerically solved) for a given a_L.

3. Discussion

An example of the solution of the new turbine array model is shown in figure 2 to illustrate the effects of a_L on the local and global power coefficients, C_{PL} and C_{PG}. In this example, the local blockage is relatively high ($B_L = 0.436$) but the array blockage is moderate ($B_A = 0.3$, i.e. 30 % of the channel span is blocked by the array). Due to the high local blockage, C_{PL} significantly exceeds the Lanchester–Betz limit of 16/27 (for a turbine in an unconfined flow) and peaks at a high induction factor (compared to the unconfined flow case, where 1/3 is the optimal induction factor to maximize the power coefficient). As a_L increases, however, C_{TL} and C_{TA} both increase and therefore the array induction factor a_A also increases (i.e. the flow through the array is reduced). Hence C_{PG} is lower than C_{PL} and peaks at an induction factor of only slightly higher than 1/3 in this case.

An interesting question here is how C_{PG} varies depending on the intra-turbine spacing. Figure 3 shows an example of the effects of s/d on the C_{PG} versus a_L curve (*a*) and on its peak value, C_{PGmax} (*b*). (Note that the results for $s/d < 0$ included on (*b*) are only mathematically meaningful as, in practice, the intra-turbine spacing cannot be negative.) The values of C_{PL} and $(1 - a_A)^3$ at the optimal a_L (that yields C_{PGmax} for each s/d case) are also plotted for comparison; note that C_{PG} is identical to the product of C_{PL} and $(1 - a_A)^3$. Here w/nd and h/d are the same as those for figure 2 and hence the global blockage is also the same ($B_G = 0.131$); however, the local and array blockages vary depending on s/d. As can be seen from figure 3, in this example, C_{PGmax} increases as s/d is reduced from 4 to ∼0.4 but then decreases as s/d is further reduced. This is because C_{PL} increases whilst $(1 - a_A)^3$ decreases as s/d is reduced. In other words, the optimal intra-turbine spacing is determined by the

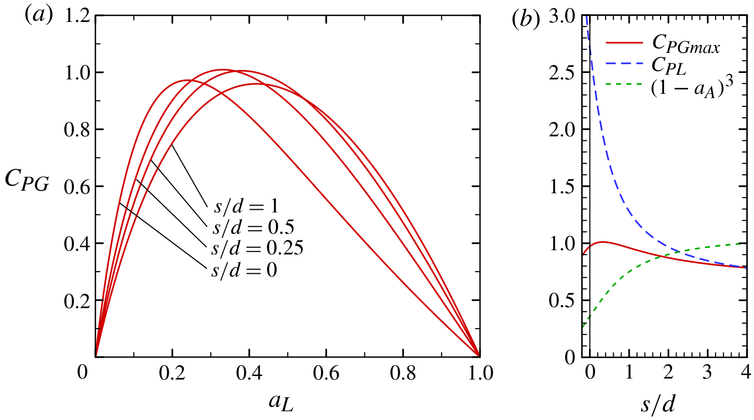

FIGURE 3. (Colour online) Effects of the normalized intra-turbine spacing s/d: on C_{PG} (*a*) and on its maximum value (*b*) ($w/nd = 5$, $h/d = 1.2$, $B_G = 0.131$).

balance between the local cross-sectional blockage effect, represented by C_{PL}, and the array-scale choking effect, represented by $(1 - a_A)^3$.

It should be noted that the present tidal array model reduces to the original model of Garrett & Cummins (2007) in the limiting cases where $s/d = w/nd - 1$. In the above example, $s/d = 4$ corresponds to this limiting case where a large number (n) of turbines are homogeneously arrayed across the entire channel of $w/nd = 5$. In such a case, the local and global power coefficients are identical since the array induction factor a_A is always zero, i.e. the array-scale (horizontal) flow expansion does not take place.

Figure 4 shows the effects of s/d and h/d on C_{PGmax} for four different channel width cases ($w/nd = 2$, 5, 10 and 100). For $w/nd = 2$ (where $0.5 \leqslant B_A \leqslant 1.0$, depending on s/d), the optimal spacing exists only when h/d is very small; for $h/d > 1.3$, C_{PGmax} continues to increase as s/d is reduced to zero. For $w/nd = 5$ (where $0.2 \leqslant B_A \leqslant 1.0$, depending on s/d), however, the optimal spacing exists for $h/d < 1.7$. This seems to be within the range of practical interest: for example, if we plan to install 30 turbines of $d = 20$ m in a wide channel cross-section of $w = 3$ km ($w/nd = 5$) and $h = 30$ m ($h/d = 1.5$), the present model predicts the optimal spacing of $\sim$2 m ($s/d = 0.1$). As w/nd further increases, the optimal spacing for each given h/d increases and the effect of h/d on the peak of C_{PGmax} diminishes.

A more comprehensive view of the variation of C_{PGmax} is provided in figure 5, where contours of C_{PGmax} are plotted with respect to the local and global blockages, B_L and B_G. Note that B_L becomes identical to B_G (and this is the minimum possible B_L) when turbines are homogeneously distributed across the channel span (i.e. $s/d = w/nd - 1$), whilst the maximum blockage (which is achieved when $s/d = 0$) depends on h/d, as indicated by the dashed lines. The white line represents the locus of the maximum power (maxima of C_{PGmax}) for given B_G, showing that the optimal local blockage increases as the global blockage is increased. For all global blockages there is advantage in clustering turbines over a homogeneous distribution.

For an infinitely wide channel ($w/nd \rightarrow \infty$), C_{PGmax} depends solely on B_L rather than on the combination of s/d and h/d, as shown in figure 6(*a*). As the local blockage B_L is increased, C_{PGmax} increases from the Lanchester–Betz limit of 0.593 (at $B_L = 0$) to another limiting value of 0.798 (at $B_L \approx 0.40$), but then decreases as B_L

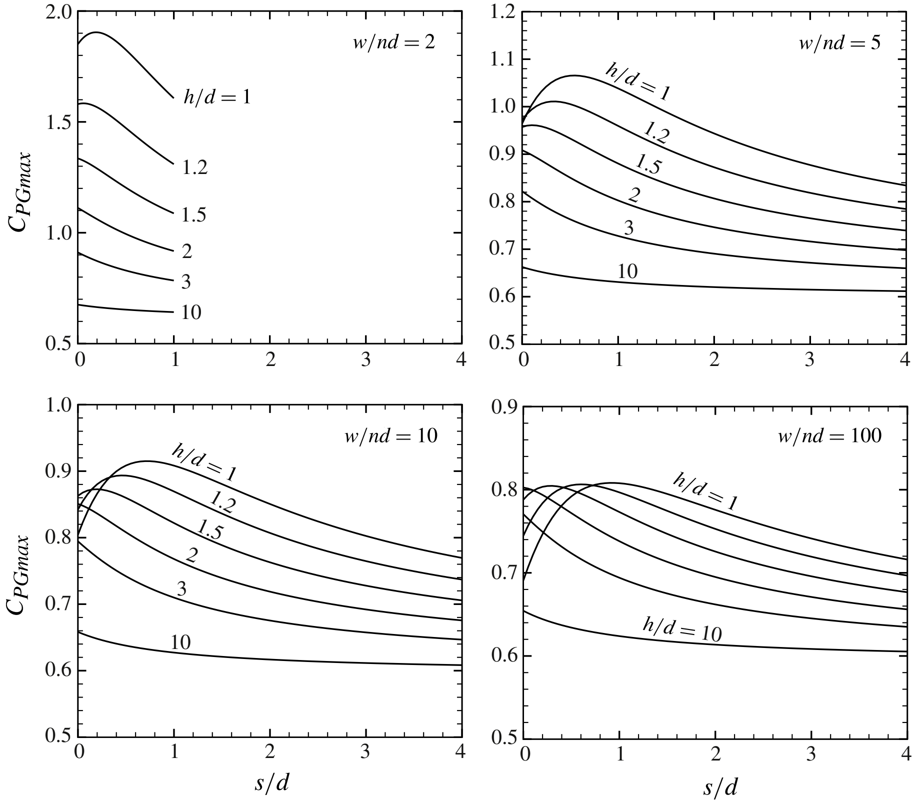

FIGURE 4. Effect of s/d and h/d on C_{PGmax}: for $w/nd = 2$, 5, 10 and 100.

is further increased. The new limiting value of C_{PGmax} can be considered as a limit of power extraction for turbine installations with finite local blockage but deployed in effectively infinite channel widths. Note that under the condition $w/nd \to \infty$ the resistance induced by the installation of turbines will be negligible compared to other flow resistances through a real channel (e.g. bed resistance). Hence the assumption that the mass flux through the channel is unaltered by the installation of the array is valid for such channels. The practical significance of this case is for headland sites where the channel stretches semi-infinitely from the shoreline.

Last but not least, it should be borne in mind that C_{PGmax} discussed above is not the only measure to assess the efficiency of a tidal fence/farm. Another important measure is the ratio of the power extracted by the turbines to the power removed from the flow (rather than to the power available). This ratio is often referred to as 'basin efficiency' in order to distinguish it from the efficiency represented by the power coefficient, and is identical to $(1 - a_G)$ for the present study:

$$\frac{\text{power extracted}}{\text{power removed}} = \frac{nP_D}{nT_D U_C} = \frac{U_D}{U_C} = (1 - a_G). \tag{3.1}$$

This means that the basin efficiency decreases as the global induction factor a_G increases. Note that $(1 - a_G) = (1 - a_L)(1 - a_A)$, i.e. increases in local and array induction factors, a_L and a_A, both contribute to an increase in a_G and thus a decrease in basin efficiency. Figure 6(b) shows the values of these three induction factors that

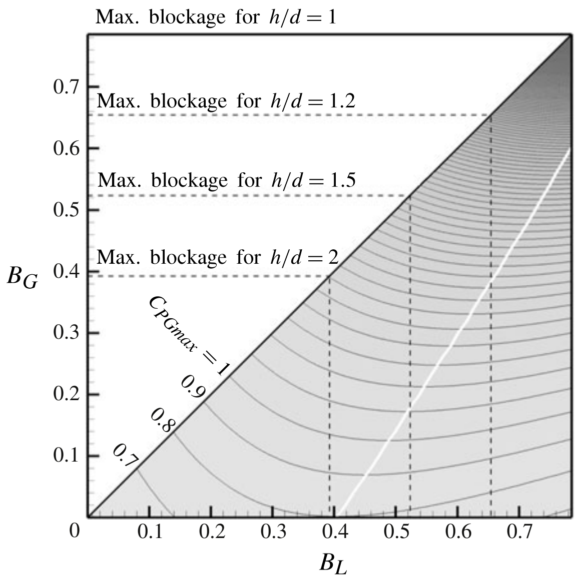

FIGURE 5. Combined effects of B_G and B_L on C_{PGmax}. White line represents the locus of the maximum power for given B_G.

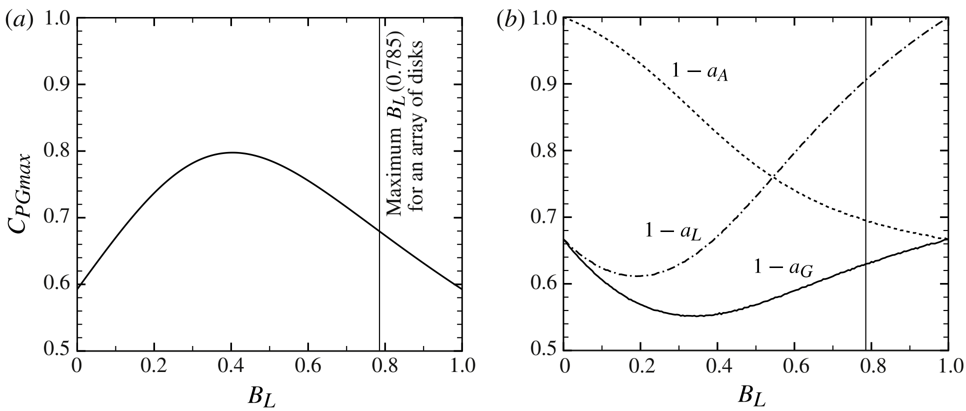

FIGURE 6. Effects of B_L on C_{PGmax} (*a*) and on the axial induction factors to achieve C_{PGmax} for given B_L (*b*): for $w/nd \to \infty$.

are required to achieve C_{PGmax} plotted in figure 6(*a*). As the local blockage B_L is increased, the basin efficiency (to achieve C_{PGmax} for a given B_L) slightly decreases from 2/3 for the Lanchester–Betz case (at $B_L = 0$) to 0.55 (at $B_L \approx 0.33$) and then it recovers as B_L is further increased. It should be noted, however, that this decrease in basin efficiency is the outcome of maximizing C_{PG}; in practice, we may operate tidal turbines at a more sensible condition such that C_{PG} is slightly lower than C_{PGmax} so as to maintain a higher basin efficiency. Figure 7 shows combined effects of B_L and the basin efficiency $(1 - a_G)$ on C_{PG} (again for $w/nd \to \infty$). It can be seen that for a fixed

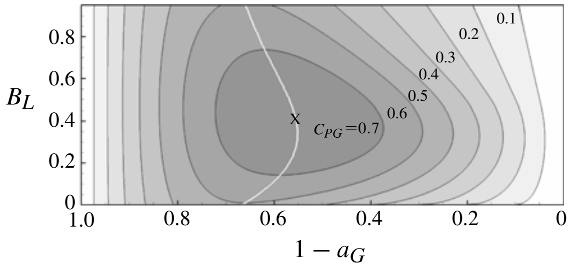

FIGURE 7. Relationship between global power coefficient (C_{PG}) and basin efficiency ($1 - a_G$) as a function of local blockage (B_L): for $w/nd \to \infty$. White line represents the locus of C_{PGmax} and $\times$ indicates the peak of C_{PG} (0.798).

high basin efficiency, for example $(1 - a_G) = 0.7$, C_{PG} still increases as B_L is increased up to $\sim$0.4.

4. Conclusions

A new theoretical model is proposed to explore the efficiency of a long array of tidal turbines partially blocking a wide channel cross-section. An idea of scale separation was introduced between the flow around each device (or turbine) and that around the entire array to assume that all device-scale flow events, including the 'far-wake' mixing behind each device, take place much faster than the horizontal expansion of the flow around the entire array. This assumption made it possible to model the flow around a long array of tidal turbines as a combination of two quasi-inviscid problems of different scales, in both of which the conservation of mass, momentum and energy was considered following the model of Garrett & Cummins (2007).

The new model provides fundamental physical insight into the efficiency of a partial tidal fence, specifically the effects of channel width, height and intra-turbine spacing (note, however, that the effect of changes in water depth was not considered in this study; hence the results for very high local blockage cases, such as $h/d \approx 1$ and $s/d \approx 0$, should be considered hypothetical). When the turbines block only a small portion of the span of a shallow channel cross-section, there is an optimal intra-turbine spacing to maximize the efficiency (limit of power extraction). The efficiency increases as the spacing is reduced to the optimal value due to the local blockage effect, but then decreases as the spacing is further reduced due to the array-scale choking effect, i.e. reduced flow through the entire array. When the turbines block a rather large portion of the channel span and/or when the channel is not shallow relative to turbine diameter, the efficiency monotonically increases as the intra-turbine spacing is reduced to zero. Also, when the channel is infinitely wide, the efficiency depends solely on the local blockage B_L rather than the combination of the intra-turbine spacing and the channel height. As B_L is increased, the efficiency increases from the Lanchester–Betz limit of 0.593 (at $B_L = 0$) to another limiting value of 0.798 (at $B_L \approx 0.40$), but then decreases as B_L is further increased.

Acknowledgements

The authors gratefully acknowledge the support of the Oxford Martin School, University of Oxford, who have funded this research.

REFERENCES

DRAPER, S., HOULSBY, G. T., OLDFIELD, M. L. G. & BORTHWICK, A. G. L. 2010 Modelling tidal energy extraction in a depth-averaged coastal domain. *IET Renew. Power Gener.* **4**, 545–554.

GARRETT, C. & CUMMINS, P. 2005 The power potential of tidal currents in channels. *Proc. R. Soc. Lond.* A **461**, 2563–2572.

GARRETT, C. & CUMMINS, P. 2007 The efficiency of a turbine in a tidal channel. *J. Fluid Mech.* **588**, 243–251.

HOULSBY, G. T., DRAPER, S. & OLDFIELD, M. L. G. 2008 Application of linear momentum actuator disc theory to open channel flow. *Tech. Rep.*. OUEL 2296/08, Dept. Engineering Science, University of Oxford.

NISHINO, T. & WILLDEN, R. H. J. 2012 Effects of 3-d channel blockage and turbulent wake mixing on the limit of power extraction by tidal turbines. *Int. J. Heat Fluid Flow*, (in press) http://dx.doi.org/10.1016/j.ijheatfluidflow.2012.05.002.

VENNELL, R. 2010 Tuning turbines in a tidal channel. *J. Fluid Mech.* **663**, 253–267.

VENNELL, R. 2011 Tuning tidal turbines in-concert to maximize farm efficiency. *J. Fluid Mech.* **671**, 587–604.

WHELAN, J. I., GRAHAM, J. M. R. & PEIRÓ, J. 2009 A free-surface and blockage correction for tidal turbines. *J. Fluid Mech.* **624**, 281–291.